

We are IntechOpen, the world's leading publisher of Open Access books Built by scientists, for scientists

6,900

Open access books available

186,000

International authors and editors

200M

Downloads

Our authors are among the

154

Countries delivered to

TOP 1%

most cited scientists

12.2%

Contributors from top 500 universities



WEB OF SCIENCE™

Selection of our books indexed in the Book Citation Index
in Web of Science™ Core Collection (BKCI)

Interested in publishing with us?
Contact book.department@intechopen.com

Numbers displayed above are based on latest data collected.
For more information visit www.intechopen.com



Comparison between Semiempirical and Computational Techniques in the Prediction of Aerodynamic Performance of the Rotor of a Quadcopter

Andres Mauricio Pérez Gordillo

Additional information is available at the end of the chapter

<http://dx.doi.org/10.5772/intechopen.69730>

Abstract

Unmanned aerial vehicle (UAV) is a growing technology used in different industries, and the main platform used for the UAVs is the quadcopter. The rotor of a quadcopter typically operates at low to moderate Reynolds number, so that the aerodynamics and an early prediction of the performance of the propellers are important in the design of the quadcopter. In the present chapter, the performance of a commercial propeller used in quadcopters is analyzed with three different techniques: momentum theory, blade element theory, and computational fluid dynamics. By applying the momentum and blade element theory, it was possible to estimate the thrust generated for a propeller in hover. A computational model based on computational fluid dynamics (CFD) was implemented and used to simulate a propeller in hover; the model predicts the wake and the thrust of the propeller as well. The results of the theory and computational approximations were compared with experimental measurements of flying tests.

Keywords: momentum theory, blade element theory, CFD, lift coefficient, figure of merit, thrust

1. Introduction

The increasing use of the unmanned aerial vehicles (UAVs) in different industries has led to the development of the common platforms used in the design of UAVs. The preferable of these platforms is the quadrotor due to its advantages such as an easier control in flight for drone

operators, a rapid takeoff, and maneuverability. In the design of a quadcopter, it is necessary to estimate the performance of the propellers used in the vehicle. This chapter presents two of the simplest and more used theories to achieve a preliminary approximation to the performance of the selected propeller; also, a CFD model is used to study the aerodynamics of a commercial propeller used in a quadcopter of the Colombian company ADVECTOR.

Momentum theory is the simplest theory to study a propeller. A propeller produces thrust by the acceleration of the column of air that passes through the rotor plane, and with the use of the laws of conservation of mass, momentum, and energy, it is possible to obtain a relation of the induced velocity from the propeller to the air and the thrust that the air produces on the propeller [1].

Blade element theory applies the aerofoil theory to the rotating blade [1], this theory studies the forces actuating in a two-dimensional (2D) section of the blade; thus, it is necessary to have a detailed description of the geometry of the blades of the propeller. It includes both the blade chord and the pitch angle distributions along the blade span; the lift and drag coefficients are assumed to be known or can be estimated for each section of the blade. The integration of the contributions of the sections along the radius yields the total thrust and torque.

The research community has been studying quadcopters in the last years, most of them developing control systems for these vehicles, but the aerodynamic effects of the rotorcraft vehicles have been often ignored [2]. The wake of a rotorcraft has a significant effect on the overall flow field and on the performance of the vehicle. The wake is characterized by induced velocities and regions with intense vortical flow which interact with rotor blades and fuselages [3]. Using computational fluid dynamics (CFD), it is possible to analyze the rotor wake and tip vortices and also to predict the performance of the propeller.

2. Momentum theory

The simplest theory to estimate the performance of a propeller is the momentum theory. This model uses an ideal fluid, that is, the air is incompressible, not viscous and irrotational, whereas the propeller is modeled as a disc with the same area that is described by the rotation of the propeller. This disc produces a pressure jump uniformly distributed to the flow passing through it [1]. **Figure 1** shows the sketch of the model.

Applying the Bernoulli equation to the fluid before the disc,

$$p_{\infty} = \frac{1}{2} \rho v_i^2 + p_i \quad (1)$$

where ρ is the air density, v_i is the velocity induced by the disc to the fluid, p_i is the pressure just before the disc, and p_{∞} is the pressure of the undisrupted fluid. Now applying Bernoulli after the disc,

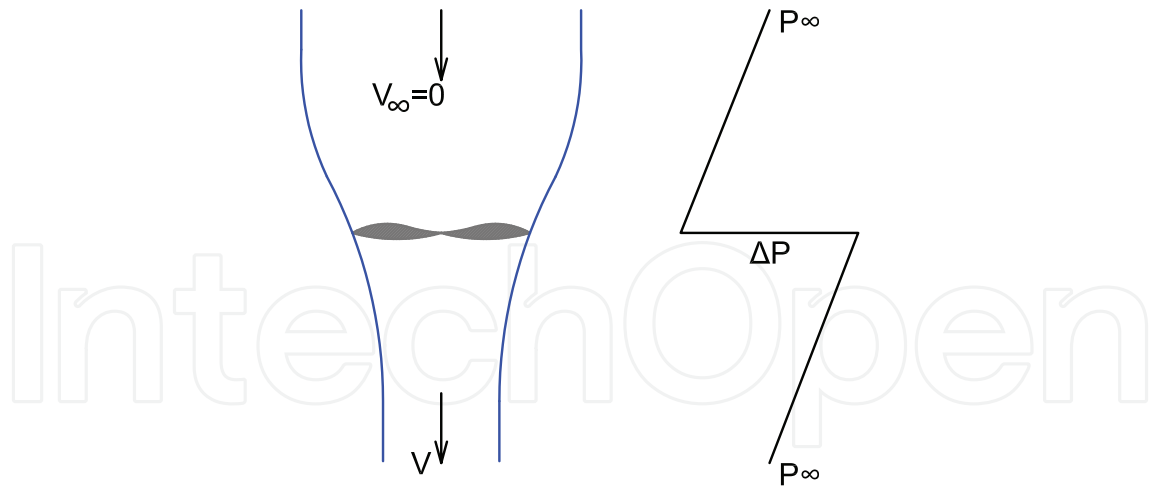


Figure 1. Disc simplification for momentum theory.

$$\frac{1}{2}\rho v_i^2 + p_i + \Delta p = p_\infty + \frac{1}{2}\rho v_\infty^2 \quad (2)$$

where v_∞ is the velocity at downstream infinity, see **Figure 1**. From Eqs. (1) and (2),

$$\Delta p = \frac{1}{2}\rho v_\infty^2 \quad (3)$$

But,

$$T = \Delta p \cdot A \quad (4)$$

where T is the thrust, Δp is the pressure jump caused by the propeller, and A is the area of the disc. From Eqs. (3) and (4),

$$T = \frac{1}{2}\rho A v_\infty^2 \quad (5)$$

Using momentum conservation, it is easy to see that the total increase on the momentum of the air must be equal to the thrust, and from **Figure 1**, $v_0 = 0$, then,

$$T = \dot{m}(v_\infty - v_0) = \rho v_i A v_\infty \quad (6)$$

Using Eq. (4),

$$\Delta p = \frac{T}{A} = \rho v_i v_\infty \quad (7)$$

And with Eq. (3),

$$\frac{1}{2}\rho v_{\infty}^2 = \rho v_i v_{\infty} \quad (8)$$

$$\frac{1}{2}v_{\infty} = v_i \quad (9)$$

Which means that half of the velocity induced to the fluid is done before the propeller and half after this, therefore,

$$T = 2\rho A v_i^2 \quad (10)$$

2.1. Induced power

The power induced on the air is the change in its kinetic energy per unit of time:

$$P_i = \frac{1}{2}\dot{m}(v_{\infty}^2 - v_0^2) = \frac{1}{2}\rho v_i A v_{\infty}^2 \quad (11)$$

And using Eqs. (9) and (10),

$$P_i = T v_i \quad (12)$$

$$P_i = \frac{T^{3/2}}{\sqrt{2\rho A}} \quad (13)$$

where P_i is the induced power of the rotor, that is, it is the power that the rotor induces in the air. The relation of the induced power in hover to the total power of the rotor is called *figure of merit* (FM), and it is one of the forms to express the efficiency of a rotor in hover [4]:

$$FM = \frac{P_i}{P} \quad (14)$$

Small propellers used in the UAV's are currently capable of an FM up to 0.65 [4].

3. Blade element theory

This theory analyzes aerodynamic forces on a 2D section of a blade, in order to find the contribution of each section to the total thrust; for this, it is necessary to know the chord and pitch angle distributions along the span of the blade. The *Lift Coefficient* C_L is a known data from the lift surface of each section of the blade.

Figure 2 shows a blade of a propeller with an elementary section of blade at a distance r from the axis of the propeller, with width Δr and chord c , and **Figure 3** shows the section of blade.

The angular velocity of the propeller is Ω . The velocity components in the section are as follows:

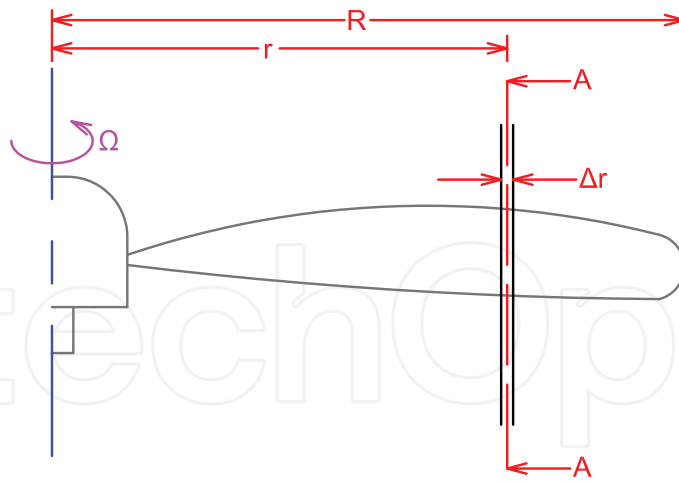


Figure 2. View of a blade.

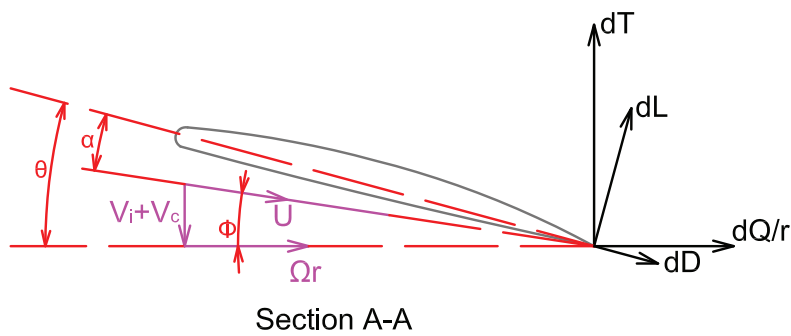


Figure 3. Details of the section of blade.

$$V_2 = \Omega r \quad (15)$$

$$V_0 = v_i + V_c \quad (16)$$

$$U = \left[(v_i + V_c)^2 + (\Omega r)^2 \right]^{1/2} \quad (17)$$

where v_i is the induced velocity and V_c is the climb velocity, see **Figure 3**. r is the radii of the section, see **Figure 2**.

The blade pitch angle is θ , and the inflow angle ϕ is calculated as

$$\phi = \tan^{-1} \left(\frac{v_i + V_c}{\Omega r} \right) \quad (18)$$

But assuming that ϕ is small, then

$$\phi = \frac{V_0}{V_2} = \frac{v_i + V_c}{\Omega r} \quad (19)$$

The incidence angle of the blade section is α

$$\alpha = \theta - \phi \quad (20)$$

For the blade section, the lift and drag forces are

$$\Delta L = \frac{1}{2} \rho U^2 c C_L \Delta r \quad (21)$$

$$\Delta D = \frac{1}{2} \rho U^2 c C_D \Delta r \quad (22)$$

where ρ is the density, c is the chord of the section, C_L and C_D are the lift and drag coefficients for the section, respectively, and Δr is the width.

From **Figure 3**,

$$\Delta T = \Delta L \cos \phi - \Delta D \sin \phi \quad (23)$$

$$\Delta Q = (\Delta L \sin \phi + \Delta D \cos \phi) r \quad (24)$$

where ΔT and ΔQ are the thrust and torque for the section of blade, respectively.

If ϕ is small,

$$\Delta T = \Delta L \cos \phi \quad (25)$$

With Eq. (21), ΔT for one blade is

$$\Delta T = \left(\frac{1}{2} \rho U^2 c C_L \Delta r \right) \cos \phi \quad (26)$$

Or for many blades

$$\Delta T = \left(\frac{1}{2} \rho U^2 c C_L \Delta r \right) B \cos \phi \quad (27)$$

where B is the number of blades of the propeller.

For a thin section, C_L could be estimated as [5]

$$C_L = 2\pi\alpha \quad (28)$$

As in the momentum theory, it is necessary to use momentum conservation in the axial direction, that is, that the change in the moment of the fluid is equal to the thrust of the blade. For a section of blade in hover,

$$\Delta T = \rho 2\pi r V_0 (V_\infty) \Delta r \quad (29)$$

But from the momentum theory, Eq. (9):

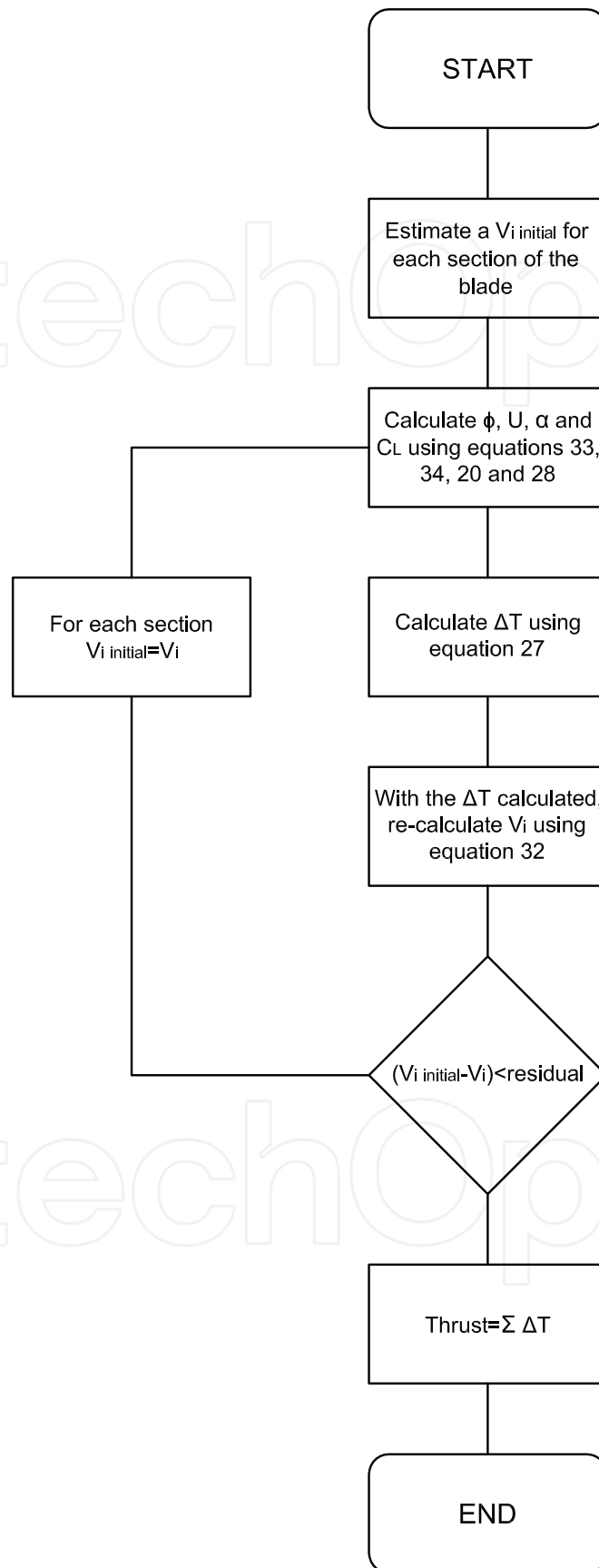


Figure 4. Method of solution using the blade element theory.

$$V_\infty = 2v_i \quad (30)$$

$$\Delta T = \rho 2\pi r V_0 (2v_i) \Delta r \quad (31)$$

But remembering that for hover $V_c = 0$, thus $V_0 = v_i$ therefore

$$\Delta T = \rho 4\pi r v_i^2 \Delta r \quad (32)$$

And Eqs. (17) and (19) become

$$U = \left[v_i^2 + (\Omega r)^2 \right]^{1/2} \quad (33)$$

$$\phi = \frac{v_i}{\Omega r} \quad (34)$$

The solution method using the blade element theory requires detailed information about the geometry of the blade, that is, subdivide the blade in many sections of small width, and for each section, measure the pitch angle θ and the chord c . With Eq. (20) and Eqs. (27), (28), (32)–(34), it is possible to solve the thrust and the v_i for a propeller in hover, but it is necessary to implement an iterative method to achieve the solution. **Figure 4** shows a flow diagram describing the iterative method of solution.

4. Computational method

This study was performed using the multiple reference frame (MRF) model in steady state. The conservative equations for a MRF for an incompressible flow are [6]

$$\nabla \cdot \vec{v}_r = 0 \quad (35)$$

$$\rho \left[\frac{\partial \vec{v}}{\partial t} + (\vec{v}_r \nabla \vec{v}) \right] + \rho (\vec{\Omega} \times \vec{v}) = -\nabla p + \nabla \bar{\tau} + \vec{F} \quad (36)$$

where \vec{v}_r is the relative velocity, $\vec{\Omega}$ is the rotational velocity (which must be constant), and in this case the Coriolis and centripetal accelerations are into a single term $\vec{\Omega} \times \vec{v}$. Many problems permit the entire computational domain to be referred to as a single rotating reference frame (SRF) [6].

Two turbulence models have been widely used to model external flows over airfoils, wings, and rotors; these models are Spalart-Allmaras and $k-\omega$. In wall-bounded flows, the vorticity and the strain are of similar magnitude, but this is not true in a vortex core where the vorticity is high, but the strain is low. In these models, the turbulence production term is based on the velocity gradient; to include the effects of rotation, it is necessary to have some modifications to the classical models.

Many authors have studied the effect of the turbulence model used in the CFD simulations of rotors [7–10]. But though many models have been used, the Spalart-Allmaras model is the most used model to simulate rotors; this is a one equation model that solves a modeled transport equation for the turbulent viscosity [11]

$$\frac{\partial}{\partial t}(\rho\tilde{V}) + \frac{\partial}{\partial X_i}(\rho\tilde{V}U_i) = G_V + \frac{1}{\sigma\tilde{V}} \left\{ \frac{\partial}{\partial X_j} \left[(\mu + \rho\tilde{V}) \frac{\partial\tilde{V}}{\partial X_j} \right] + C_{b2} \left(\frac{\partial\tilde{V}}{\partial X_j} \right)^2 \right\} - Y_V + S\tilde{V} \quad (37)$$

where \tilde{v} is the modified turbulent viscosity, G_v is the production of turbulent viscosity, Y_v is the destruction of turbulent viscosity that occurs in the near-wall region, $\sigma\tilde{v}$ and C_{b2} are the constants of the model, ν is the molecular kinematic viscosity, and $S\tilde{v}$ is a source term. More information about how to calculate the terms in Eq. (37) and the constants of the model can be found in Ref. [11].

A drawback of the Spalart-Allmaras model is that this model is insensitive to streamline curvature and system rotation [6]. A modification to the turbulence production term is available to sensitize this model to the effects of streamline curvature and system rotation. An empirical function is used as a multiplier of the production term to account for these effects; detailed information can be found in Ref. [12].

The simulations were performed using the CFD software ANSYS FLUENT v17.0. The turbulence model used in the model was the Spalart-Allmaras model with curvature correction; the SIMPLE pressure-velocity coupling solver was used, with second-order upwind discretization for convective and diffusive terms. The simulations were performed increasing the rotational velocity with small discrete steps starting with 1 rpm up to a maximum velocity of 6547 rpm. For each increase in angular velocity, the model was run until the variation of residuals was very small; in this case, the convergence criteria were adjusted to 1×10^{-6} . The working fluid is air at the conditions of the experimental test; see Section 5 of this chapter.

4.1. Geometry and computational domain

The actual rotor blade installed in the quadrotor model Araknos V2 of the Colombian company ADVECTOR is used for this study. A three-dimensional (3D) scanning was performed to obtain a CAD of the propeller; see **Figure 5**.

The diameter of the propeller (DP) is 360 mm, the root chord is 20.77 mm, the tip chord is 4.33 mm, and the chord at 75% of span is 25.31 mm. The computational domain is a vertical cylinder, with 3.3 DP in diameter and 7 DP in length; the propeller is centered in the domain and at 2.7 DP from the upper surface. The generated mesh is an unstructured grid of tetrahedral elements but with a refined grid of pyramidal elements near the propeller surface.

The simulations were performed on the server clustergate of Universidad de los Andes, with Intel X86_64 processors with a velocity of 2.4 MHz using 32 cores and 64 GB of RAM memory. The simulation for the final grid took 168 h (**Figure 6**).



Figure 5. CAD model of the propeller.

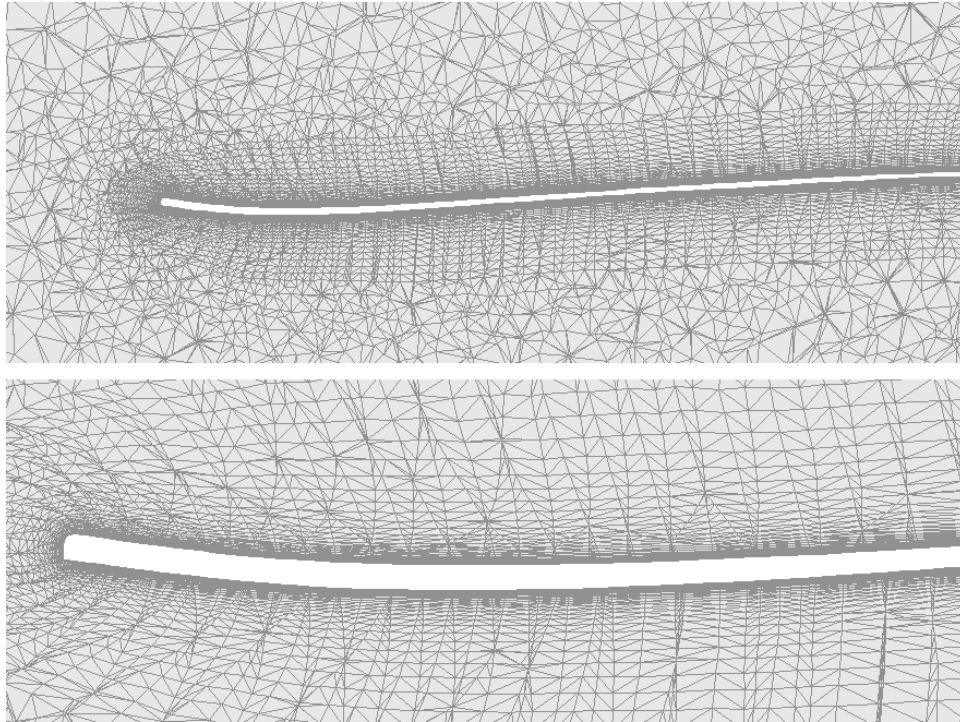


Figure 6. Mesh. Up: general mesh around the propeller; down: pyramidal elements near the wall.

A grid convergence analysis was performed using different meshes with total number of elements varying from 0.8 to 16 million cells. Total torque was used as convergence criteria at 5221 rpm. It was found that for an increase of the number of elements from 9.6 to 16.5 million, the change in the force predicted was 0.2%; it was concluded that the mesh with 9.6 million cells was sufficient.

The boundary conditions for the upper and lateral surface of the cylinder are set as pressure inlet, while the lower surface is set as a pressure outlet and the propeller boundary is a non-slip wall.

5. Experimental methodology

Flight test was performed with the quadcopter ARAKNOS V2, see **Figure 7**; the flying test was in hover at a height of 15 m from the ground, with an atmospheric pressure of 748 hPA and an average temperature of 24°C. Power for the motors was supplied only from one battery,



Figure 7. Multirotor Araknos V2 used in this study.

whereas other batteries were used as ballast. These flights were monitored using the software Mission Planner, which provided real-time information on battery voltage and control output to the engines. Flight data collected from the IMU, barometer, voltage and current sensor, and control output were recorded by the autopilot and downloaded for analysis. The data of rotational speed and electrical power recorded during hovering flight were analyzed.

The main features of the motor used in the quadcopter are as follows:

- Out runner.
- Brushless.
- kV: 530 rpm/V.
- Rotor diameter: 50 mm
- Rotor height: 10 mm.
- Shaft diameter: 3.17 mm.
- Inner resistance: 127 m Ω .
- No load current: 0.5A at 7990 rpm and 14.8 V.

6. Results

6.1. Experimental measurements

The test was performed at an average velocity of 4430 rpm, the air density was 0.87 kg/m³, and the power measured in the motor was $P = 62.7$ W, achieving a thrust of $T = 5.89$ N.

6.2. Momentum theory

As indicated in Ref. [4], the FM for the early propellers used in UAVs was in the range of 0.4–0.45; now, the currently used propellers in these vehicles develop FM up to 0.65. With this consideration, a conservative value of $FM = 0.5$ was estimated for the propeller used in the quadcopter ARAKNOS, including the loss in the motor but without the loss of power in the coupling propeller-motor shaft, because this is a fixed coupling with screws.

From Eq. (14), it is possible to obtain the value of the induced power, taking the value of power measured in the flight test $P = 62.7$ W.

$$P_i = 31.35 \text{ W} \quad (38)$$

The diameter of the disc is 0.36 m and the air density is $\rho = 0.87 \text{ kg/m}^3$, with these data and using Eq. (13):

$$T = 5.58 \text{ N} \quad (39)$$

The value obtained with this model is close to the measured value. It was necessary to assume the FM for the propeller.

6.3. Blade element theory

To apply the blade element theory, it was necessary to split the blade of the propeller in sections with a $\Delta r = 1$ mm, and for each section measure the chord (c) and the pitch angle (θ).

As explained in **Figure 4**, it is necessary to give an initial guess to v_i for each section of the blade; for simplicity, a uniform-induced velocity along the span of the blade was used as the initial value of v_i for the iterative process.

The initial guess of v_i is important because if the iterative method is simple, this could not converge and would be necessary to apply some techniques for convergence as, for example, Crank-Nicholson or under-relaxation [5].

A simple iterative code was written in Matlab to solve the thrust using the blade element theory, and the initial value of v_i was estimated using the momentum theory. Using the value of thrust obtained from the momentum theory and with Eq. (10),

$$v_i = 5.61 \text{ m/s} \quad (40)$$

The code needs the values of the radii, the chord, and the pitch angle for each section; also, it is necessary to indicate the rpm, in this case 4430 rpm; the density of the fluid; the width of the section; the number of blades; and the initial guess for v_i .

Adjusting the maximum residual of v_i to 1×10^{-4} , the result of the code is

$$T = 5.07 \text{ N} \quad (41)$$

Seventy-one iterations were necessary to achieve the convergence of the method.

The thrust estimated using the blade element theory is close to the thrust measured in the experimental tests. Thought the iterative method was simple, it was easy to achieve convergence; this was possible thanks to the use of the momentum theory to estimate the initial value of v_i . From the results of the code, it was possible to see that even when the initial guess for v_i was considered as uniform along the span of the blade, the final distribution of the induced velocity is not uniform, in the root of the blade $v_i = 3.7$ m/s while at 75% of the span $v_i = 5.8$ m/s and at the tip $v_i = 2.96$ m/s.

6.4. Computational results

Figure 8 shows the wake developed by the propeller at 4500 rpm; the criterion to visualize the vortex is the Q -criterion with a threshold of 200, and the structure of the wake is similar to that described in Ref. [1], where it is clear that the strong vortex is created at the tip of the blade, also the tip vortex and the inner vortex descend below the rotor following a helical path.

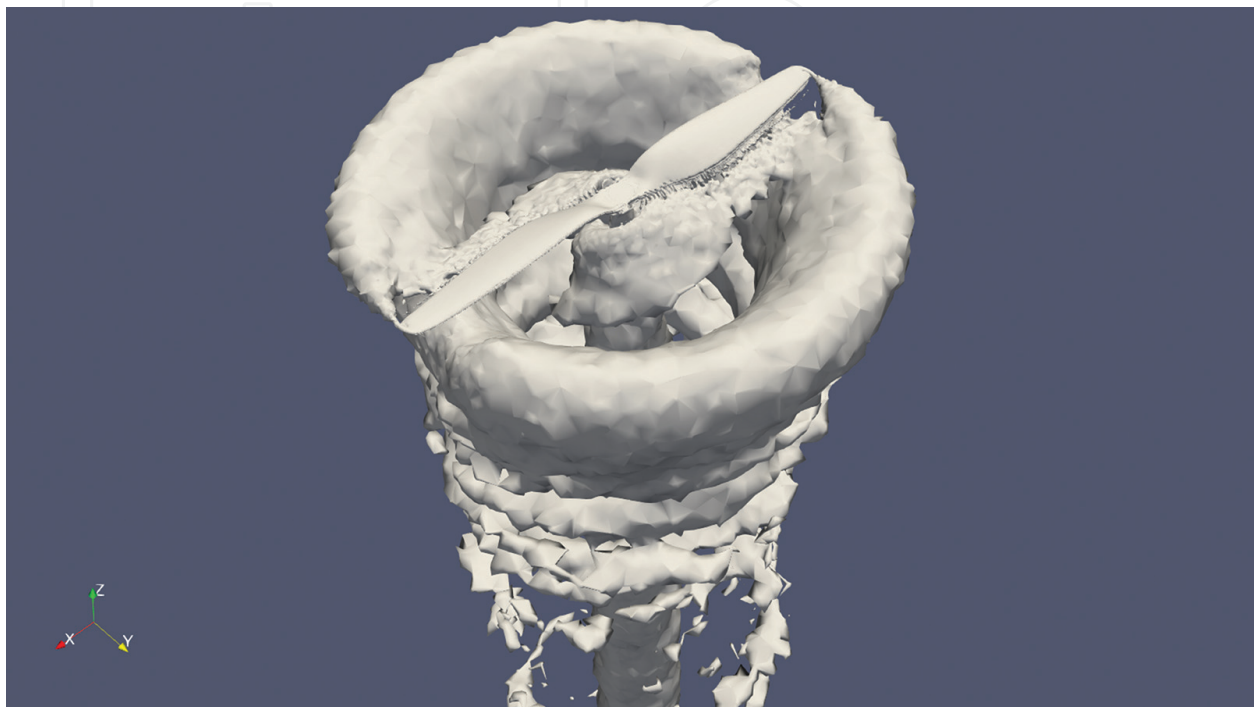


Figure 8. Vortex Contours at 4500 rpm using Q -criterion with a threshold of 200.

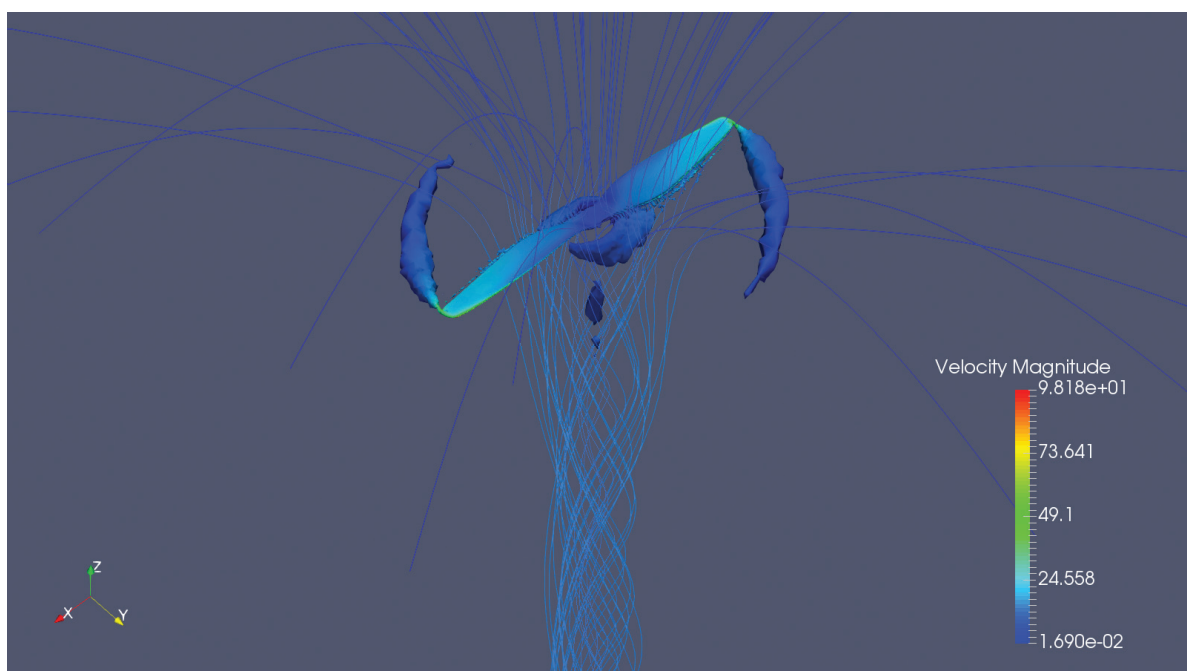


Figure 9. Streamlines colored by velocity magnitude and contours of Q -criterion = 50,000, at 4500 rpm.

There are various methods used to visualize vortex; some of these methods are based on the tensor gradient of velocity as, for example, the Q -criterion and λ_2 -criterion; other methods are based on vorticity, for example, the magnitude of vorticity, there are some Lagrangian methods as direct Lyapunov exponents (DLE) or the Mz criterion; more information about the methods to visualize vortex structures could be found in Ref. [13].

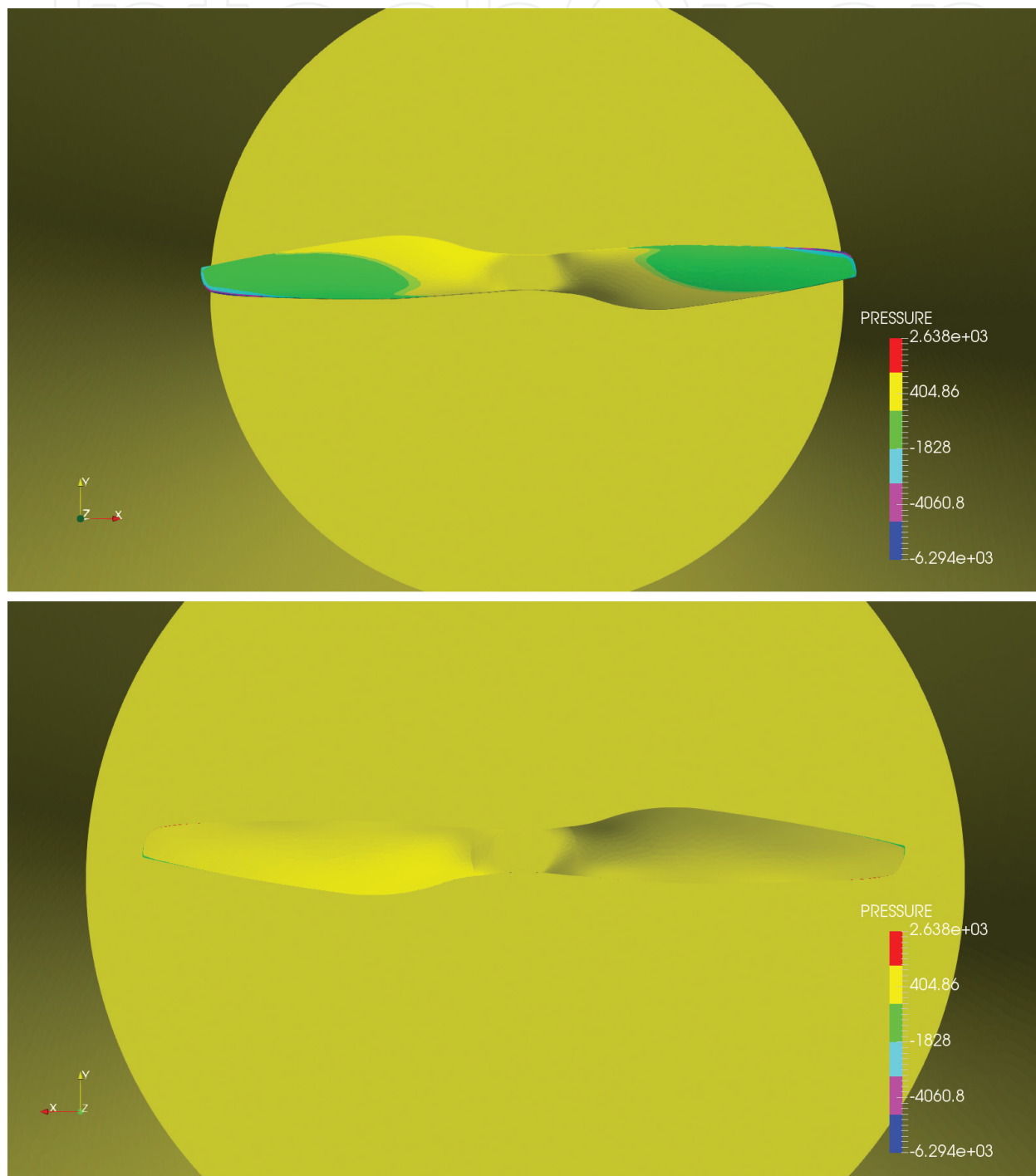


Figure 10. Contours of pressure on the surfaces of the propeller in PA at 4500 rpm, up upper surface, down lower surface.

Figure 9 shows streamlines colored by velocity magnitude and the vortex contours with a threshold for Q -criterion of 50,000; the model shows the increase of the magnitude of the velocity down the propeller, also the streamlines swirl around the axis of the propeller.

Figure 10 shows the contours of pressure for the upper and lower surfaces of the propeller. As expected, the pressure is lower at the upper surface of the propeller.

Finally, the thrust predicted by the model is

$$T = 6.99 \text{ N} \quad (42)$$

The model is able to predict the wake, pressure, velocity fields, and thrust of the propeller at hover and for different operational rotational velocities using the MRF method in steady state. The model overpredicts the thrust; this difference could be due to the interaction of the four rotors between them and also with the fuselage of the aircraft in the experimental measurements.

7. Conclusions

The momentum and blade element theories are useful tools to achieve a preliminary estimation on the performance of a propeller in hover, though it is important to understand the strong simplifications that each of these theories imply. For the momentum theory, simplifications are strong, for example, the flow is ideal, the simplification of the disc implies that the propeller has an infinite number of blades, also the induced velocity is uniform along the span of the propeller, and for the solution it was necessary to estimate the efficiency of the propeller in hover; this could lead to unrealistic results. For the blade element theory, the first simplification is that the flow is studied as a 2D flow, and effects of a 3D flow are ignored, for example, the induced velocities by the tip vortex, also linear aerofoil properties are used for the sections of the blade, that is, to estimate C_L . The method does not simplify the induced velocity as being uniform along the blade; instead it is possible to estimate the induced velocity distribution for the propeller in hover.

A CFD model was implemented to study the flow around a propeller in hover. The model is able to predict the wake, pressure, velocity fields, and thrust using the MRF method in steady state. The predicted wake is in agreement with the literature.

The theoretical approximations for thrust are closer to the measurement of the experimental test, while the computational method overestimates the thrust. **Table 1** shows that the maximum percentage of error is 18.7% for the CFD simulation.

For a better validation of the models analyzed in this chapter, a test bench to a more accurate measurement of thrust is necessary.

Method	Experimental	Momentum theory	Blade theory	Computational simulation
Thrust [N]	5.89	5.58	5.07	6.99
Error		5.3%	13.9%	18.7%

Table 1. Comparison of the results with the experimental measurement.

The control of a quadcopter is based on the thrust and torque of the propulsion system; therefore, an adequate estimation of the aerodynamic parameters is very important for the control of the vehicle. The methods described have some characteristics that are important to apply in some of the stages of the design, for example, the momentum theory is important for a first estimation of the size of the rotor; **Table 2** shows the advantages and disadvantages of each method.

Method	Advantages	Disadvantages
Momentum theory	<ul style="list-style-type: none"> • Simple method • First estimation of propeller aerodynamic performance (thrust torque) • With this approximation it is possible to size a rotor for a given power 	<ul style="list-style-type: none"> • Strong suppositions • It does not account for number of blades • It does not concern the details of the flow around the blades • It is not useful to design the rotor because it does not account the shape of the blade • It is an ideal fluid theory
Blade theory	<ul style="list-style-type: none"> • The model allows studying the shape of the blade, and therefore it possible to design the rotor • The mathematical solution is no complex and not computationally expensive 	<ul style="list-style-type: none"> • The model simplifies the blade to 2D non-interacting sections • It is necessary to estimate the C_L distribution of the blade • It is an ideal fluid theory
Computational simulation	<ul style="list-style-type: none"> • It is a real fluid method • It is possible for a more detailed study of the structure of the flow • It is a 3D method • It allows the verification of the results of the other methods 	<ul style="list-style-type: none"> • High computational cost • It is a complex method

Table 2. Benefits and limitations of each method.

Acknowledgements

The authors like to thank the Departamento Administrativo de Ciencia, Tecnología e Innovación Departamento (COLCIENCIAS) and its program to sponsor PhD students in Colombia, also to the high-performance computing center at Universidad de los Andes for providing the computational resources, and ADVECTOR for being part of this research, sharing their technical data and to perform the necessary flying tests.

Nomenclature

A	Area of the disc
c	Chord
C_D	Drag coefficient
C_L	Lift coefficient
D	Drag
FM	Figure of merit
L	Lift
P_i	Induced power of the rotor

p_i	Pressure just before the disc
p_∞	Pressure of the undisrupted fluid
Q	Torque
T	Thrust
V_c	Climb velocity
v_i	Induced velocity
v_∞	Velocity at downstream infinity
Δp	Pressure jump caused by the propeller
ρ	Density
θ	Blade pitch angle
ϕ	Inflow angle
α	Incidence angle

Appendix

Matlab code for blade element theory.

```

%*****
%% It is necessary to load the vectors of
% Radii r [ m] , Chord c [ m] and Pitch Angle theta [ rad]
%*****
%*****
%% Data
%*****
rpm=4430;% Rotational velocity rpm
omega=rpm*2*pi/60;% Rotational velocity [ rad/s]
rho=0.87;% Density [ kg/m^3]
dr=0.001;% Delta r [ m]
B=2;% # blades
Vi=5.61;% Initial guess for Vi [ m/s]
%*****
%% Initial Velocities
%*****
vi0=zeros (length (r) ,1);
vi0=vi0+Vi;% Vector of initial vi [ m/s]
v2=r.*omega;% Vector of V2 [ m/s]
%*****
%% Iterative method
%*****
Rmax=10;% Residual
n=0;% Iteration Counter
while Rmax>0.0001;

```

```

U=((vi0.^2)+(v2.^2)).^0.5;% U [ m/s]
fi=vi0./v2;% Angle fi [ rad]
alfa=theta-fi;% Angle of inflow [ rad]
Cl=alfa.*(2*pi);% Lift Coefficient
DT=((((U.^2)*0.5*rho).*c).*Cl).*dr*B).*cos(fi);% Differential of Thrust
[ N]
vi=((DT./(rho*4*pi*dr))./r).^0.5;% New Vi [ m/s]
R=vi0-vi;% Residual of Vi
R=abs(R);
Rmax=max(R);
n=n+1;
vi0=vi;
end
THRUST=sum(DT)
Residual=Rmax
Iteraciones=n

```

Author details

Andres Mauricio Pérez Gordillo

Address all correspondence to: am.perez259@uniandes.edu.co

Universidad de los Andes, Bogotá, Colombia

References

- [1] Seddon J. Rotor in vertical flight: Momentum theory and wake analysis. In: Basic Helicopter Aerodynamics. 1st ed. BSP Professional Books, Great Britain: 1990
- [2] Hoffmann G, Huang H, Waslander S, Tomlin C. Quadrotor helicopter flight dynamics and control: Theory and experiment. AIAA Guidance, Navigation and Control Conference and Exhibit. 20 - 23 August 2007, Hilton Head, South Carolina. AIAA 2007-6461
- [3] Potsdam M, Pulliam T. Turbulence Modeling Treatment for Rotorcraft Wakes. US Army Research, Development, and Engineering Command, NASA Ames Research Center. AHS specialists conference on aeromechanics. San Francisco, CA, 2008
- [4] Pereira JL. Hover and wind-tunnel testing of shrouded rotors for improved micro air vehicle design [dissertation]. University of Maryland, College Park; 2008. p. 349
- [5] Auld, Srinivas. Aerodynamics for Students [Internet]. 1995-2016. Available from: <http://s6.aeromech.usyd.edu.au/aerodynamics/index.php/sample-page/propulsion/blade-element-rotor-theory/> [Accessed: January 10, 2017]

- [6] ANSYS Inc. ANSYS FLUENT 12.0/12.1 Documentation [Internet] 2009. Available from: <http://www.afs.enea.it/project/neptunius/docs/fluent/index.htm> [Accessed: September 20, 2016]
- [7] Lazaro C, Poroseva S. Computational analysis of the blade number effect on the performance of a ducted propeller. In: AIAA Atmospheric Flight Mechanics Conference; January 5–9, 2015; Kissimmee, FL: American Institute of Aeronautics and Astronautics; 2015
- [8] Gomez S, Gilkey L, Kaiser B, Poroseva S. Computational analysis of a tip vortex structure shed from a bio-inspired blade. In: AIAA Applied Aerodynamics Conference; June 16–20, 2014; Atlanta: American Institute of Aeronautics and Astronautics; 2014
- [9] Duraisamy K, Baeder JD. High resolution wake capturing methodology for hovering rotors. *Journal of the American Helicopter Society*. 2007;52(2):110–122
- [10] Doerff P, Szulc O. Numerical Simulation of Model Helicopter Rotor in Hover. Institute of Fluid-Flow Machinery PAS. *TASK Quarterly : scientific bulletin of Academic Computer Centre in Gdansk*. 2008;12(3-4): 227–236
- [11] Spalart P, Allmaras S. A One-Equation Turbulence Model for Aerodynamic Flows. American Institute of Aeronautics and Astronautics Technical Report; 30th Aerospace Sciences Meeting and Exhibit, Reno, NV, U.S.A., 1992
- [12] Spalart P, Shur ML. On the sensitization of turbulence models to rotation and curvature. *Aerospace Science and Technology*. 1997;1(5): 297–302
- [13] Holmen V. Methods for vortex identification [dissertation]. Master's Theses in Mathematical Sciences. Mathematics (Faculty of Technology) and Numerical Analysis. lund university libraries 2012. p. 46

IntechOpen

